The temperature wave method of determining fracture toughness values due to crack propagation

D. G. MONTGOMERY
*Department of Civil Engineering, Wollongong University College,
New South Wales, Australia*

A method is presented of determining fracture toughness by measurement of the amount of heat emitted at the tip of a propagating crack. Two thermojunctions placed adjacent to the crack were used to monitor the temperature wave produced at fracture. An electromagnetic fluxmeter was used to integrate the thermojunction output with respect to time and was calibrated to give a direct reading in terms of strain energy release rate G. The temperature wave method is independent of initial crack length and fracture surface area and can be readily used for specimens having complex sections. Values obtained by this method compare favourably with toughness values determined by a linear elastic fracture mechanics analysis. Results of static and dynamic three-point bending tests on specimens at different temperatures within the range -40 to $60°$ C are reported.

Notation

a	= distance between thermojunctions
a_0	= initial crack length
a'	= radius of disc heat source
c	= specific heat
e	= base of Napierian logarithm
k	= thermal conductivity
q	= plane source strength for temperature wave
s	= standard deviation
t	= time
t_0	= time to maximum temperature
t_R	= time of fluxmeter reading after fracture
x	= distance from heat source to measurement point
x_0	= distance from heat source to first thermojunction
x_1	= distance from heat source to second thermojunction
B	= specimen thickness
E	= modulus of elasticity
G, G_1	= strain energy release rate or crack extension force; subscript 1 refers to opening mode of crack extension.
G_C, G_{IC}	= critical value of G or G_1 at point of instability of crack extension
K, K_1	= stress-intensity factor of elastic stress field in vicinity of crack front;

	subscript 1 refers to opening mode of crack extension
K_C, K_{IC}	= critical value of K or K_1 at point of instability of crack extension
L	= half-span length
N	= non-dimensional time
P	= load at fracture
T	= temperature rise
$\bar{T}$	= temperature difference
T'	= temperature gradient at time t
T_0	= temperature rise at first thermojunction
T_{x_0}	= temperature at first thermojunction
T_1	= temperature rise at second thermojunction
T_{x_1}	= temperature at second thermojunction
W	= specimen width
α	= thermal diffusivity of material
β	= variable in correction factor for temperature wave method
ν	= Poisson's ratio
ρ	= density
σ	= variance
σ_{ys}	= yield stress
ϕ	= temperature time flux
$\phi_{(tR)}$	= fluxmeter reading at time t

1. Introduction

Fracture toughness testing methods have existed for many years, the toughness values normally being calculated using knowledge of the load at fracture and intrinsic specimen dimensions. Irwin [1] generalized the Griffith's theory of fracture to formulate the strain energy release rate G. This progressed to the concept of crack tip stress intensity factor K which has been successfully applied to the analysis and prediction of fracture toughness in notched specimens.

Many experiments have been carried out to determine transition temperature ranges in steels which exhibit sharp changes in toughness level at certain temperatures. For some time after notched specimen tests came to be used for the assessment of transition temperatures in steels and fabricated structures, small specimens were used, without correction for the section thicknesses used in practice. In modern practice, where the use of thick sections has become more widespread, it is realized that representative transition temperatures for structures can be reliably measured only in specimens embodying full section thicknesses.

Most fracture mechanics testing methods are rigidly controlled by certain parameters, the principal one being that conditions of either plane stress or plane strain should exist in the test piece. Linear elastic fracture mechanics analyses depend on accurate knowledge of the specimen parameters, especially initial crack depth and area of fracture surface, and require a knowledge of the stress analysis of the specimen.

It is proposed that the temperature wave method can be employed to obtain fracture toughness values in specimen configurations not readily suitable to the linear elastic fracture mechanics approach.

Owing to the fact that the method is calibrated directly in terms of energy per unit area of fracture surface, it permits measurement of the actual work rate when a crack passes a fixed point beside which a thermocouple is placed, therefore overcoming the problem of variable initial crack depth, particularly where the crack may initiate in damaged material of low toughness and propagate into parent material of increased toughness. The method does not depend on either plane stress or plane strain conditions being entirely dominant, is independent of fracture surface area and can be used to determine fracture toughness for specimens of complicated

shape which inhibit the use of normal stress analyses.

Contained in this paper is an analysis of the temperature wave theory applied to fracture toughness measurements. Experimental results were obtained using an electromagnetic fluxmeter which was calibrated directly in terms of strain energy release rate G. Results of tests on three-point bend specimens tested throughout a temperature range of $100°$ C are presented, comparisons between the toughness values obtained using the temperature wave method and a linear elastic fracture mechanics approach being shown.

2. Temperature wave theory

2.1. Use of temperature wave to measure surface energy

Wells [2, 3] made use of a simple thermocouple and mirror galvanometer system to measure the surface energy due to fracture. This method made use of the relationship [4] that approximately 90% of the energy formed by plastic work at a crack tip is evolved as heat, the remainder of the energy of plastic flow being stored as potential energy of strain in the crystal lattice.

The source of heat at a flat running crack could be considered as an instantaneous plane source giving pure one-dimensional heat flow because of the high relative speed of a brittle fracture compared to the speed of a temperature wave travelling through a metallic material.

Assuming the source strength to be q heat units per unit area, produced instantaneously, Carslaw and Jaeger [5] show that the temperature rise T, above that of the surroundings, at any time t after release and at distance x from the plane of the source is:

$$T = \frac{q.e^{-x^2/(4\alpha t)}}{2\rho c \sqrt{(\pi \alpha t)}} \qquad (1)$$

where α is the thermal diffusivity (related to the thermal conductivity, k, by $\alpha = k/\rho c$), ρ is the density and c is the specific heat of the material.

The maximum temperature reached, at distance x, is

$$T_{max} = \frac{q}{\rho c x \sqrt{(2\pi e)}} \qquad (2)$$

and occurs after a time t_0, where

$$t_0 = \frac{x^2}{2\alpha}. \qquad (3)$$

The temperature rise T was measured by a thermocouple located at distance x from the plane of the crack.

2.2. Modified temperature wave theory

The method of measurement is simplified [6] and made more sensitive by integrating the thermocouple measurements with respect to time through the use of a directly connected electromagnetic fluxmeter, which is essentially an integrating voltmeter having a torsion-string mechanism with practically total restoring-force compensation. The integral of the temperature rise equation (Equation 1) with respect to time, is:

$$\int_0^t T.\mathrm{d}t = \frac{q}{\rho c}\left[\left(\frac{t}{\pi\alpha}\right)^{\frac{1}{2}}.e^{-x^2/(4\alpha t)} - \frac{x}{2\alpha}\,\mathrm{erfc}.\frac{x}{\sqrt{(4\alpha t)}}\right]. \quad (4)$$

Non-dimensional plots of the temperature rise equation and its integral (both for plane source) versus time are shown in Fig. 1. The temperature wave, in theory, does not become zero until an infinite time has elapsed. To enable a finite reading to be obtained by the electromagnetic fluxmeter, two thermojunctions located close together were considered.
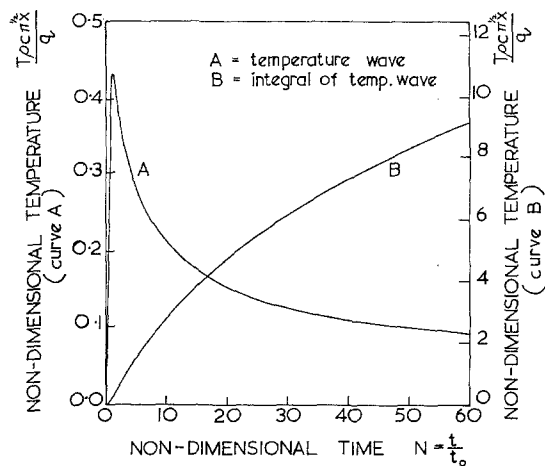
Figure 1 Non-dimensional plot of temperature rise equation and its integral: plane source.

Considering two thermojunctions, the first (equivalent hot junction) at a distance x_0 and the second (equivalent cold junction) at a distance x_1 from the plane fracture face, it follows from first principles that

$$G_C = 2k\int_0^\infty T'.\mathrm{d}t \quad (5)$$

where T' is approximated by $\bar{T}/a$, and $\bar{T}$ is the temperature difference between hot and cold junctions. a = distance between thermojunctions, i.e. $a = x_1 - x_0$; G_C = fracture toughness in thermal units; k = thermal conductivity of the material; t = time elapsed since fracture. The temperature difference between the thermojunctions is proportional to the voltage difference measured by the thermojunctions. Equation 5 can be rewritten as:

$$\phi = \frac{G_C.a}{2k} \quad (6)$$

where ϕ is the total amount of temperature-time flux registered by the electromagnetic fluxmeter.

This relationship is for infinite time; however, due to limitations in the construction of the fluxmeter and its sensitivity, it is necessary to incorporate a correction factor for use in measuring the temperature flux evolved in a given finite time. The modified equation is:

$$\phi_{(tR)} = \frac{G_C.a}{2k}\left(1 - \frac{\beta+1}{\beta-1}\cdot\frac{a}{2\sqrt{(\pi\alpha t_R)}}\right) \quad (7)$$

where $\phi_{(tR)}$ = fluxmeter reading at time t_R; $\beta = (x_0 + a)/x_0$; t_R = time of fluxmeter reading after instant of fracture. Details of the derivation of the modified heat equation are given in the Appendix.

Non-dimensional plots of the temperature rise equations, exact and approximate (Equation 7) solutions to the integral of their difference and the integral at infinity for thermojunctions placed close together are shown in Fig. 2.

3. Calibration of fluxmeter and the temperature wave method

3.1. Test rig and theory

A simple and rapid method of calibrating the electromagnetic fluxmeter to give results directly in terms of energy without involving fracture tests was devised. A rig was developed which produced instantaneous plane sources of heat comparable to those produced at the fracture face in a steel specimen. Frictional heat was developed at the slightly domed vertical end faces of a circular cross-section steel rod, supported horizontally in matching steel cups. The rod was transiently rotated by the drop of an off-centre mass, attached by a member in the plane perpendicular to the centre-line of the rod.
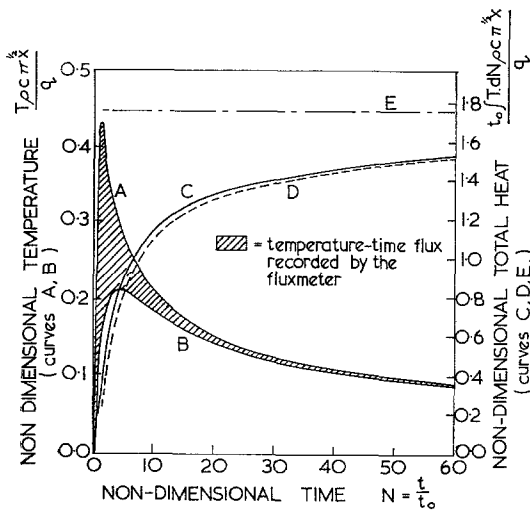
Figure 2 Non-dimensional plot of temperature rise equations and integral of their difference for thermojunctions close together.

Input energy was calculated using the height of drop of the mass. The temperature wave was detected by a pair of thermojunctions peened in the surface of the rod, adjacent to one end and at distances of 10 and 20 mm from the vertical end face.

Carslaw and Jaeger indicate that the temperature rise T at time t for a disc source is:

$$T = \frac{q}{2\rho c \sqrt{(\pi \alpha t)}} \cdot \left[1 - e^{-(a')^2/(4\alpha t)} \right] \cdot e^{-x^2/(4\alpha t)}$$

(8)

where a' is the radius of the disc source and x is the distance between the heat source and the measuring point.

Due to the relatively small diameter of the bar, plane transient heat flow theory was used to analyse the results. Because the distance between the thermojunctions and the interface was in excess of the radius of the bar ($x > 2a'$ for the apparatus), any irregularities due to non-uniform heat generation with respect to the radius of the bar were insignificant and Equation 8 reduces to the equation of temperature rise from an instantaneous plane source (Equation 1).

208

3.2. Results

Nine series of tests were performed, each containing an average of twenty-five different input energies. For each input energy the fluxmeter scale deflections were recorded at five second intervals, ranging from zero to 60 sec.

Plots of input energy versus fluxmeter reading at times of 5, 15 and 60 sec are shown in Fig. 3. Scatter of results increases with time, this being the result of random drift of the fluxmeter. Plots of fluxmeter reading, and standard deviation from the theoretical and practical mean versus time of reading are shown in Fig. 4. It can be seen that the theoretical and practical fluxmeter reading against time curves are coincident, and there is a well defined least standard error of 0.055, at a reading time of 16 sec. This indicates that the most suitable time to read the fluxmeter, and hence minimise errors due to drift, occurs at a time of sixteen seconds after formation of the temperature wave.
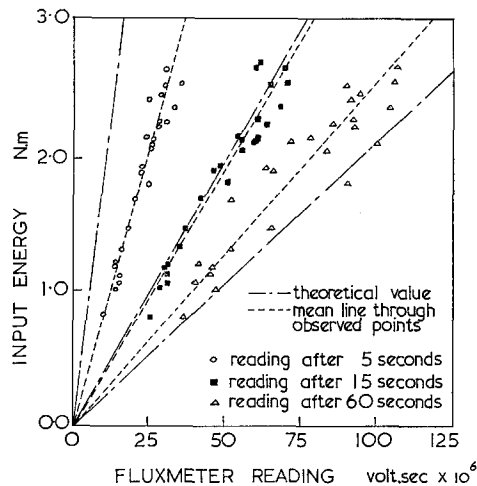
Figure 3 Input energy as a function of fluxmeter reading.

Substituting the values for steel into Equation 7 and using these results for thermojunction distances a and x_0 both 10 mm, the fluxmeter can be calibrated directly in terms of crack extension force G_C and stress intensity factor K_C (plane stress, where $K_C = \sqrt{(EG_C)}$) as shown in Fig. 5. Under these conditions, for steel, the fluxmeter calibration is $G_C = 31.1$ kN m^{-1} ($K_C = 80.2$ MN m$^{-\frac{3}{2}}$) for 100 divisions on the most sensitive scale (i.e. scale factor 5×10^{-6} V sec). The correction factor (Equation 7) at the optimum time is approximately 0.5. The results

where   A = theoretical fluxmeter reading/time curve
        B = average practical fluxmeter reading/time
            curve
        C = standard deviation from practical mean
        D = standard deviation from theoretical mean
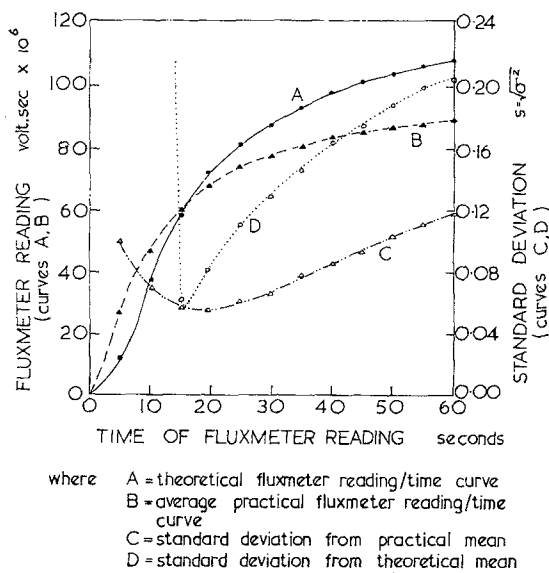
Figure 4 Theoretical and average practical fluxmeter reading and standard deviation as functions of time of fluxmeter reading.
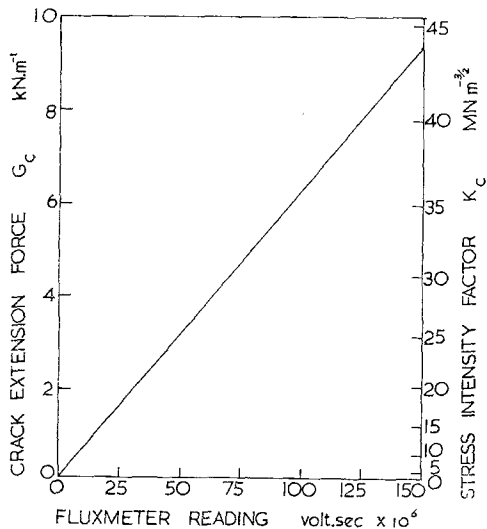
Figure 5 Crack extension force and stress intensity factor as functions of fluxmeter reading.

take into account the 90% conversion efficiency of work of plastic deformation to heat.

4. Experimental technique

A number of machines were designed and constructed, including three separate test rigs to enable specimens to be both fatigue cracked and tested in static and dynamic bending. Mild

steel specimens having cross-sections 51 mm square and 76 mm square were tested by three-point bending within a temperature range -40 to $+60°$ C.

Tests were performed, both by slow-loading and by impact, to check the validity of the temperature wave method in the linear elastic range. Temperature wave results were compared with toughness values obtained using a linear elastic fracture mechanics analysis proposed by Srawley and Brown [7].

All specimens contained a Charpy notch (45° included angle) machined transverse to the longitudinal axis and at mid span of each specimen. The notch was machined to a depth 20% of specimen depth and root radius 0.254 mm The 51 mm square specimens, each 457 mm long, were cut from a bright cold-rolled mild steel bar. The specimens were tested in three-point bending, span length between supports being 229 mm. The 76 mm square specimens were cut to a length of 380 mm and tested in bending with a span length of 305 mm. All specimens were fatigue cracked for a depth of approximately 5 mm below the notch tip.

The specimens were instrumented with thermocouple wires, positioned at longitudinal distances of 10 and 20 mm from the expected plane of cracking, to provide readings of the temperature rise evolved at fracture. Steel-constantan thermocouple circuits were employed, the materials being 28 s.w.g. constantan thermocouple wire with the steel specimen being used to complete the circuit.

The thermojunctions were mounted on the vertical specimen surface, transverse to the notch axis, the constantan wires being inserted and peened in 0.635 mm diameter holes, drilled to a depth of 2.5 mm. The wires were encased in epoxy resin to provide rigidity at their point of emergence from the surface. Protective plastic tubing surrounded the wires which were connected to terminal blocks mounted on the specimen surface, adjacent to the positions of the thermojunctions. Heavy protected wires were connected between the terminal blocks and the measuring instruments.

Specimen temperatures at the time of fracture were recorded by an electronic thermometer attached to each specimen adjacent to the crack. The e.m.f. produced by the thermojunctions was measured using the fluxmeter.

The slow-loading tests were performed in a testing rig incorporating a 270 kN capacity

hydraulic jack. Load deflection values were recorded on the Y-scale and X-scale, respectively, of a chart pen-recorder, the deflection being obtained by a direct current differential transformer. Impact tests were performed in a 40 kN m capacity drop weight rig.

A steel constantan thermocouple circuit was calibrated experimentally. The thermocouple circuit was connected through a potentiometer, values of e.m.f. being obtained at temperature intervals of $1°$ C, throughout a range from 25 to $80°$ C.

5. Test results and discussion

5.1. Thermocouple calibration

The steel-constantan thermocouple exhibited a linear variation of e.m.f. with temperature, the output being 45×10^{-6} V $°C^{-1}$.

5.2. Slow loading tests

5.2.1. 51 mm square specimens

Both the temperature wave method and linear elastic fracture mechanics approach results were calculated for plane strain conditions using the equation:

$$K_{IC} = \frac{\sqrt{(EG_{IC})}}{(1 - v)^2} \qquad (9)$$

where v is Poisson's ratio. Fig. 6 shows plots of stress intensity factor K_{IC} versus temperature. Values of crack extension force G_{IC} were obtained using Equation 1, modified to include a correction factor due to "heat reflections" from the specimen end boundary, which in practice nullify a portion of the value $\phi_{(tR)}$. This correction necessitated a 7% increase in the observed value of $\phi_{(tR)}$. The values of stress intensity factor were then calculated using Equation 9.

Plane strain linear elastic fracture mechanics results were obtained using the equation:

$$EG_{IC} = \left(\frac{P}{B}\right)^2 \cdot \frac{L^2}{W^3} \left[31.7 \frac{a_0}{w}\right.$$
$$\left. - 64.8 \left(\frac{a_0}{w}\right)^2 + 211 \left(\frac{a_0}{w}\right)^3\right] \qquad (10)$$

where P = load at fracture; B = specimen thickness; W = specimen depth; L = half-span length between supports; a_0 = initial crack length (machined notch and fatigue crack). All specimens were tested at a constantly increasing loading rate of 2 kN sec^{-1}, the tests requiring a time of 60 to 85 sec to produce fracture.

K_{IC} value increases marginally with increase

210
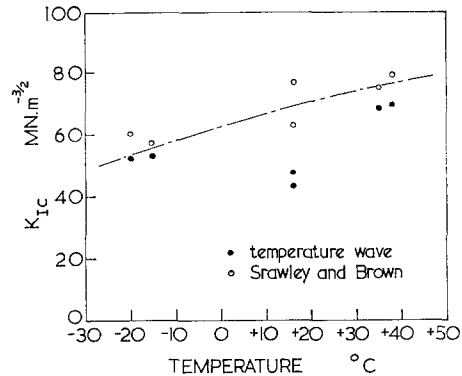
Figure 6 Stress intensity factor as a function of temperature for static bend tests on 51 mm square specimens.

in temperature. All fractures were brittle, with no shear lips being present on the fracture surface.

The two low values of K_{IC}, using the temperature wave method, were possibly due to unbalanced drift occurring in the fluxmeter. The linear elastic fracture mechanics results are generally higher; however, the analysis does not strictly apply as valid plane strain crack toughness conditions only exist for $K_{IC} \leqslant 41.6$ MN $m^{-\frac{3}{2}}$ obtained from the equation:

$$B \geqslant 2.5 \left(\frac{K_{IC}}{\sigma_{ys}}\right)^2, \text{ for valid plane strain [8]} \quad (11)$$

where B = specimen thickness = 51 mm; σ_{ys} = material yield stress = 293.7 MPa. All results calculated using Equation 10 were higher in value than the maximum value of K_{IC} for valid plane strain conditions.

5.2.2. 76 mm square specimens

Plots of stress intensity factor K_{IC} versus temperature are shown in Fig. 7. As for the 51 mm square specimens, the K_{IC} values increase with increase in temperature. Although the fractures remained brittle throughout the temperature range tested, shear lips were present in small areas on specimens tested at temperatures in excess of $+40°$ C.

The temperature wave results were calculated for plane strain conditions. The specimens were tested at a constantly increasing loading rate of 2.35 kN sec^{-1}, time of fracture occurring between 45 and 100 sec.

Valid plane strain conditions ($K_{IC} \leqslant 63.5$ MN$m^{-\frac{3}{2}}$) existed for all but one of the specimens tested. Examination of the fracture surfaces confirmed that the fatigue crack length was
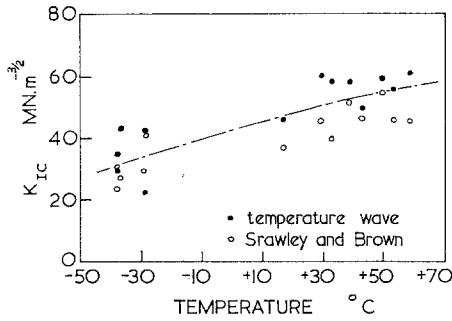
Figure 7 Stress intensity factor as a function of temperature for static bend tests on 76 mm square specimens.

extremely variable across the specimen width. Because the analysis using Equation 10 depends on accurate determination of initial crack length a_0, results calculated were subject to error as it was necessary to estimate average values of a_0.

5.3. Impact tests
The results of the tests are presented in Fig. 8. Stress intensity factors were calculated using the temperature wave theory for specimens tested in the temperature range $+15$ to $+60°$ C. Fractures remained brittle throughout the temperature range tested, with shear lips being present in small areas at temperatures in excess of $+40°$C. Results were calculated for plane strain conditions.

5.4. Temperature wave method as a criterion for determining fracture toughness
The method appears suitable for determining fracture toughness values for crack propagation in bend specimens. Results obtained using the
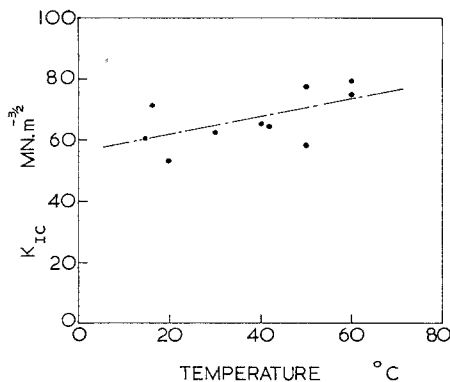
Figure 8 Stress intensity factor as a function of temperature for dynamic bend tests on 76 mm square specimens.

temperature wave method are in general agreement with those obtained using a linear elastic fracture mechanics approach. The method is of sufficient accuracy to detect the heat produced at the fracture surface (of the order of $1°$C), even when the specimens are tested throughout a temperature range of $100°$C.

In dynamic tests the temperature wave method is ideally suited where the determination of toughness values is difficult to obtain accurately by other methods.

Because the system is calibrated directly in terms of energy per unit area no measurement of fracture surface area is required. Thus the temperature wave method is particularly useful in cases where complicated specimen shapes or irregular initial crack lengths make determination of fracture toughness difficult or inaccurate by other methods.

6. Summary
A method has been devised to determine the fracture toughness of steel by measurement of the amount of heat emitted by the plastic work at the tip of a propagating crack causing fracture. The method makes use of the integral of the heat evolved with respect to time at the fracture surface in calibrating an electromagnetic flux-meter directly in terms of crack extension force.

The method was calibrated using a simple technique and temperature wave results for crack propagation were obtained for steel specimens tested in three-point bending. Specimens of two sizes were tested in impact and slow-loading conditions. The temperature wave produced at fracture was detected by two thermojunctions, constructed by inserting and peening constantan thermocouple wires in the specimen surface, located transversely at small distances from the fracture plane.

Results obtained by the temperature wave method compare favourably with toughness values determined using linear elastic fracture mechanics analysis. Specimens were tested throughout the temperature range -40 to $+60$ C.

The method is particularly suitable in cases where complex sections or irregular initial crack lengths make analysis by other methods difficult.

7. Appendix: Derivation of the modified heat equation (from Carslaw and Jaeger [5] and Wells [2])
For plane wave heat source:

211

$$T = \frac{q.e^{-x^2/(4\alpha t)}}{2\rho c \sqrt{(\pi\alpha t)}}$$

where T = temperature rise; q = source strength (heat units per unit area); t = any time after release; x = distance of measuring point from plane of source; α = thermal diffusivity of material where $\alpha = k/\rho c$ and k = thermal conductivity, ρ = density, c = specific heat.

Maximum temperature reached at distance x is:

$$T_{max} = \frac{q}{2\rho cx} \cdot \sqrt{\left(\frac{2}{\pi e}\right)} = \frac{q}{\rho cx\sqrt{(2\pi e)}}$$

and occurs at time t_0, where

$$t_0 = \frac{x^2}{2\alpha}.$$

Replacing q by G_C (crack extension force) in heat units

$$T = \frac{G_C e^{-x^2/(4\alpha t)}}{2\rho c \sqrt{(\pi\alpha t)}}$$

$$T_{max} = \frac{G_C}{\rho cx\sqrt{(2\pi e)}}, \quad t_0 = \frac{x^2}{2\alpha}.$$

If the temperature gradient at x is T' at any time t, then the heat flow rate past the plane x is kT'. In an infinite time all the heat $G_C/2$ (half of the total heat G_C goes to each side of the crack) passes through the plane and is dispersed by conduction.

$$\therefore G_C = 2k \int_0^\infty T'.dt \cdot$$

T' may be defined as

$$\frac{T_{x_0} - T_{x_1}}{x_1 - x_0}$$

where T_{x_0} = temperature at first thermojunction (or plane), distance x_0 from the crack; T_{x_1} = temperature at second thermojunction (or plane), distance x_1 from the crack. $x_1 - x_0$ = distance between thermojunctions. Therefore,

$$G_C = 2k \int_0^\infty \left(\frac{T_{x_0} - T_{x_1}}{x_1 - x_0}\right).dt \cdot$$

This reduces to

$$G_C = \frac{2k\phi}{a}$$

where $a = x_1 - x_0$; ϕ = fluxmeter reading = $\int_0^\infty (T_{x_0} - T_{x_1}).dt$. This relationship is for

infinite time; however, due to limitations in construction and sensitivity of the fluxmeter a correction factor is necessary for use in measuring the amount of heat emitted in a given finite time. To calculate correction factor:

Let $x_0 = x$, $x_1 - x_0 = a$
$x + a = \beta x$.

Temperature rise at first thermojunction

$$T_0 = \frac{G_C e^{-x^2/(4\alpha t)}}{2\rho c \sqrt{(\pi\alpha t)}}.$$

Temperature rise at second thermojunction

$$T_1 = \frac{G_C.e^{-(\beta x)^2/(4\alpha t)}}{2\rho c \sqrt{(\pi\alpha t)}}.$$

$\therefore$ Nett temperature rise $= T = T_0 - T_1$

$$= \frac{G_C}{2\rho c \sqrt{(\pi\alpha t)}} \left(e^{-x^2/(4\alpha t)} - e^{-\beta^2 x^2/(4\alpha t)}\right)$$

$$\therefore T = \frac{(\beta^2 - 1) G_C x^2}{\rho c \sqrt{\pi}(4\alpha t)^{\frac{3}{2}}}.$$

If fluxmeter is read at a certain time t_R, then a correction factor is necessary for the heat produced in the time between t_R and infinity.

$$\therefore \text{Correction factor} = \int_{t_R}^\infty T.dt$$

$$= \frac{(\beta^2 - 1) G_C.x^2}{2\sqrt{\pi}.k\sqrt{(4\alpha t_R)}}.$$

For fluxmeter, the heat equation becomes

$$\int_0^{t_R} T.dt = \int_0^\infty T.dt - \int_{t_R}^\infty T.dt$$

$$\therefore \int_0^{t_R} T.dt = \frac{G_C a}{2k} - \frac{(\beta^2 - 1) G_C.x^2}{2\sqrt{\pi}.k.\sqrt{(4\alpha t_R)}}$$

$\therefore$ Correction factor is $1 - \dfrac{(\beta^2 - 1)x^2}{2\sqrt{(\pi\alpha t_R)}a}$

but $x + a = \beta x$,
$\therefore$ correction factor becomes

$$1 - \frac{(\beta + 1)}{(\beta - 1)} \cdot \frac{a}{2\sqrt{(\pi\alpha t_R)}}$$

but fluxmeter reading $\phi_{(tR)} = \int_0^{t_R} T.dt$

$$\therefore \phi_{(tR)} = \frac{G_C a}{2k} \left(1 - \frac{(\beta + 1)}{(\beta - 1)} \cdot \frac{a}{2\sqrt{(\pi\alpha t_R)}}\right).$$

Acknowledgements

References

1. G. R. IRWIN, *Amer Soc. Metals*, Cleveland, Ohio, 1948.
2. A. A. WELLS, *Welding Research* **7** (1953) 34-r.
3. *Idem, N.E. Coast Inst. Eng. and Shipbuilders* **71** (1955) 277.
4. G. I. TAYLOR and H. QUINNEY, *Proc. Roy. Soc.* **A143** (1934) 318.
5. H. S. CARSLAW and J. C. JAEGER, "Conduction of Heat in Solids", (O.U.P., 1947) p. 219.
6. D. G. MONTGOMERY, Ph.D. Thesis, Queen's University Belfast (1970).
7. J. E. SRAWLEY and W. F. BROWN, *A.S.T.M. S.T.P.* **381** (1965) 133.
8. W. F. BROWN and J. E. SRAWLEY, *ibid* **410** (1967).